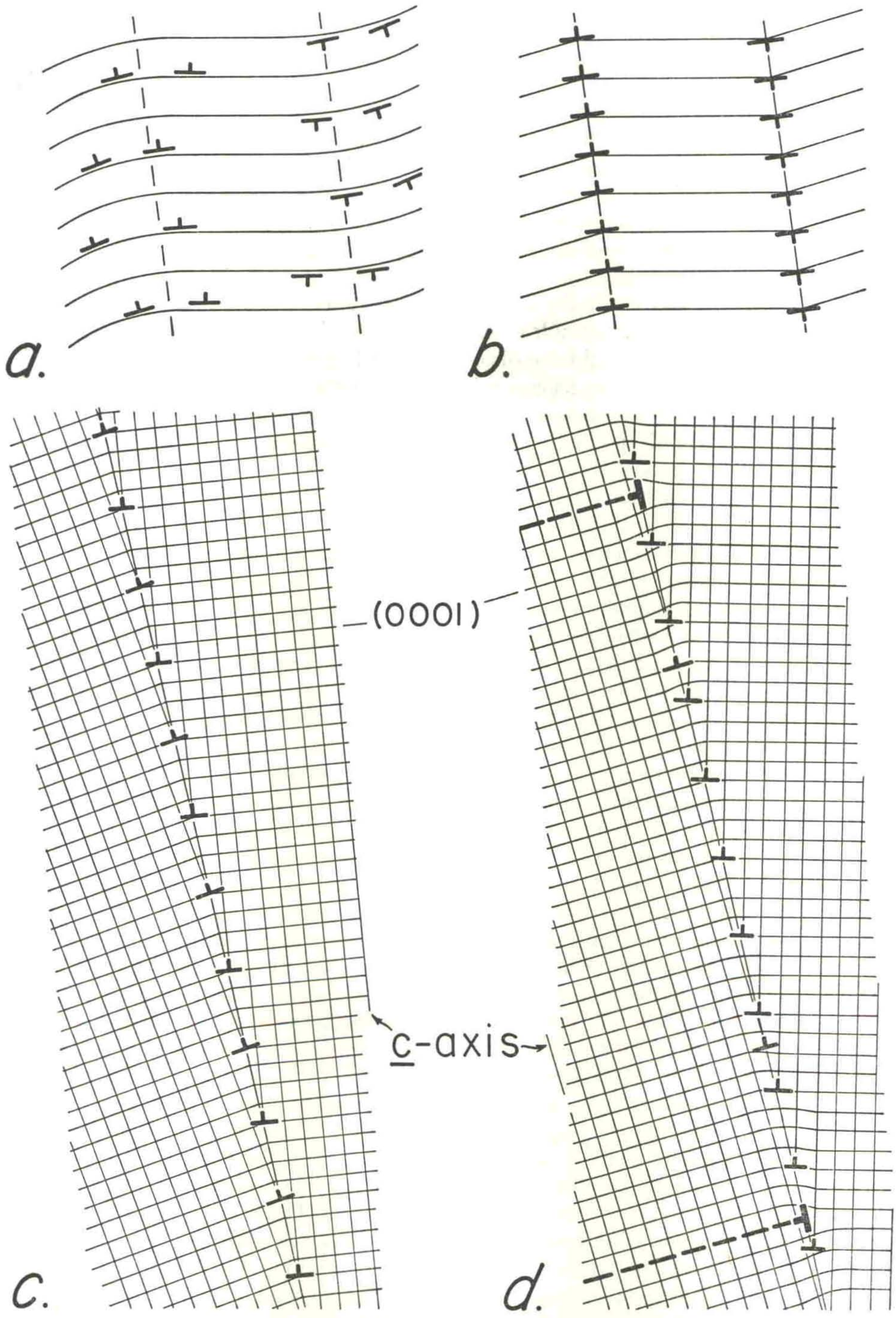

FIG. 6.—Dislocation models of band boundaries. *a*, simple deformation band showing edge dislocations of opposite sign accumulated in slip planes at opposite boundaries of a band. *b*, polygonized band boundary, showing dislocations redistributed into two walls of opposite sign at the boundaries (*a* and *b* after Cottrell, 1953, p. 166). *c*, model of a symmetrical kink boundary in quartz viewed parallel to the dislocation lines. Tilt is approximately 7° on each side of boundary. *d*, model of an asymmetrical band boundary in quartz, viewed along the dislocation lines. Tilt is approximately 2° on left side of the boundary and 12° on right. Basal edge dislocations introduce extra prism planes on each side of boundary, and prismatic edge dislocations introduce extra basal planes (*heavy broken lines*) on side with smaller tilt. (In *c* and *d* distortions of the prism planes in the neighborhood of basal edge dislocations are omitted for simplicity.) Basal and prismatic dislocation lines are assumed to be normal to the plane of the figure.

tions may become redistributed in a vertical array or "wall" in the plane of the boundary, this being a more stable arrangement (fig. 6, *b*). The latter model is identical with that of a simple grain boundary across which the disorientation is prescribed by a small rotation about an axis in the boundary.

We shall consider a model for the boundaries of *c*-axis bands in our samples consisting of such an array of basal edge dislocations (dislocations lying in the base parallel to the boundary; Burgers vectors in the base) locked in the boundaries. This is consistent with the observed strains in the bands and with the dislocation model for the basal lamellae discussed above. The sharpness of some of the band boundaries indicates that the dislocations responsible for the rotation across the boundaries are concentrated in a zone of width less than the resolving power of the microscope (*ca.* 0.2 μ or 400 lattice spacings). Electron microscopy, however, shows dislocation distributions similar to figure 6, *a* and shows that the dislocations have not formed a wall, as in figure 6, *b*. This is true for experiments at moderate temperature. At high temperature the boundaries may polygonize, but this has not yet been investigated. These two models (fig. 6, *a*, *b*) produce identical effects when viewed with an optical microscope, so for purposes of easy visualization we shall consider the boundaries as though they were polygonized.

The model in figure 6, *c* represents a symmetrical kink boundary. The edge dislocations in the wall introduce extra prismatic planes, in equal number on each side of the boundary. Chou (1962, p. 2750, Case *a*) has calculated the expressions for the stresses due to an infinite wall of uniformly spaced dislocations of this type in hexagonal crystals. All components of the stress decrease very rapidly with increase in distance from the wall and become negligible at distances greater than the spacing of the dislocations in the wall. Chou's equations are exact only for small rotations across the boundary but also hold approximately for moderate rotations of the magnitude observed in our samples (5°–30°, average 14°). For a symmetrical boundary with a total rotation of 14°, the spacing (h) of the dislocations is: $h = \frac{1}{2} b/\sin 7°$ where b is the Burgers vector of the dislocations. This gives a value for h of 20 Å, or approximately four lattice spacings; this is equivalent to a density (N) of 5×10^6 dislocations per centimeter of the boundary. Thus at distances greater than 20 Å from such a boundary the stresses are negligible, so that an array of this type should have no effect on the indices or birefringence of the quartz as observed under the microscope.

ORIGIN OF THE ASYMMETRY OF THE KINK BANDS

It is shown above that, if kink bands are formed by slip on a single system, the crystal axes will be symmetrical about the kink-band boundary except for elastic distortions. Maintenance of this symmetry as the kink band develops requires rotation of the kink-band boundary through the crystal so that it always bisects the angle between the host and the externally rotated crystal in the band. Such rotation would be accomplished in the dislocation model of figure 6, *c* by migration of the dislocations which form the kink-band boundary in their own slip planes. In order that a kink band form, however, these dislocations must have been trapped by obstacles to their motion at the kink-band boundary. These obstacles would restrict further motion and hence tend to produce the type of asymmetry which is observed.

It has been noted above that kink bands develop more readily in crystals oriented so that two *a*-axes are equally stressed ($\perp r$, $\perp z$) than when slip is preferred on one *a*-axis (0^+). It has been shown that the *a*-axis is the preferred slip direction and that slip in the $\perp r$ and $\perp z$ crystals probably occurs by simultaneous slip parallel to the two equally stressed *a*-axes. Interaction between these two slip systems may be important in trapping dislocations at the kink-band boundary.

The development of lamellae parallel to the *c*-axis is mentioned below as evidence